

Chemisorption-Site Geometry from Polarized Photoemission: Si(111)Cl and Ge(111)Cl[†]

M. Schluter, J. E. Rowe, and G. Margaritondo*
Bell Laboratories, Murray Hill, New Jersey 07974

and

K. M. Ho and Marvin L. Cohen

*Physics Department, University of California, Berkeley, California 94270, and Molecular and Materials
 Research Division, Lawrence Berkeley Laboratory, Berkeley, California 94270*

(Received 4 June 1976; revised manuscript received 31 August 1976)

The chemisorption-site geometries for chlorine on cleaved Si(111) 2×1 and Ge(111) 2×1 surfaces have been determined by comparing detailed pseudopotential calculations with energy distribution spectra and polarization selection rules of photoemission spectroscopy. Strong *p*-symmetry polarization effects observed in photoemission allow us to determine that on Si(111) the correct geometry is a onefold covalent site while on Ge(111) the Cl is in a threefold coordinated ionic site.

Previous investigations¹⁻⁵ of chemisorption on semiconductor surfaces have been interpreted *only* in terms of density-of-states effects and wave function symmetry has *not* been important. We report use of polarization selection rule effects due to two different chemisorption-site geometries on cleaved Si(111) 2×1 and Ge(111) 2×1 surfaces. The extension to other more complex adsorbate-substrate combinations is possible.⁶ The method is a combined experimental and theoretical approach⁷ similar to that used previously. Polarized synchrotron radiation is used with a wide range of photon energy, $\hbar\omega$, so that matrix elements and final-state effects can be studied with a more complete determination of valence-band density-of-states features.⁸ The other, more important new procedure is to use the two *orthogonal* polarizations at a fixed angle of incidence for the photons so that polarization selection rule effects can be *clearly separated* from possible local-field enhancement of optical matrix elements.⁹

The experimental chamber (with base pressure $\sim 6 \times 10^{-10}$ Torr) was connected to the University of Wisconsin Synchrotron Radiation Center's vertically dispersing Seya-Nanioka monochromator which had better than 98% linear polarization in the range, $\hbar\omega = 10-38$ eV, used in these experiments. By use of a differentially pumped double-sliding adapter the entire sample chamber could be rotated under ultrahigh vacuum by 90° about the incident photon beam. The angle of incidence was 45° and the electric vector of the photons was parallel (*p*) or perpendicular (*s*) to the plane of incidence. The photoelectrons were energy analyzed by a double-pass cylindrical mirror analyzer¹⁰ and standard counting electronics. The

chlorine gas was admitted through a high-purity leak valve and saturation exposures for cleaved Si(111) 2×1 were in the range $\sim 100-400$ L (1 L = 10^{-6} Torr sec) while for Ge(111) 2×1 exposures were $\sim 50-100$ L. Low-energy electron-diffraction studies⁹ show primitive (1×1) surface structures after chlorination for both Si and Ge.

Because of the large adsorbate-substrate electronegativity difference ($\Delta X \approx 1.2$) a threefold-coordinated-site geometry is probable and has been widely used for halogens chemisorbed on metal (111) surfaces.^{11,12} In this geometry the Si and Ge broken-bond electrons can be used to complete the closed-shell noble-gas configuration of Cl⁻¹. On the other hand, if electronegativity differences and closed-shell ionic configurations are *not* the dominant factors one would expect the onefold-coordinated covalent-site geometry found for hydrogen chemisorbed on Si(111) surfaces to be correct.²⁻⁴

The calculations used a self-consistent pseudopotential technique described previously.⁷ Because of the very similar electronic structures of Si and Ge the calculations were performed only for the Si(111) surface. Local model potentials for Si⁺⁴ and Cl⁺⁷ were used.^{7,13} The accuracy of the Si⁺⁴ potential has been tested in detail previously⁷ while the Cl⁺⁷ potential is less accurate and leads to a 10-20% increase in the *s-p* atomic splitting compared to experiment. This is not likely to influence the present results strongly since the Cl *s*-like states are ~ 12 eV below the Cl *p* states which interact directly with the Si valence electrons. Self-consistency is important in these calculations to treat the two geometries on an equal footing. The valence-band structure for the combined adsorbate-substrate system is

solved by an interactive technique using a periodic-layer arrangement. At each step an exact Hartree screening potential is calculated and Slater's form, $\sim \alpha\rho^{1/3}$, of the exchange and correlation interaction is used with $\alpha = 0.79$. The Cl-Si bond length chosen is 2.16 Å for the onefold covalent site (i.e., the sum of covalent radii) and 2.81 Å for the threefold site which is the sum of Si^{+1} and Cl^{-1} ionic radii. Bond length determination on the basis of chemical grounds as done here has been very successful in the past.^{1,4}

Figure 1 shows the calculated local density of states for the two geometries corresponding to a

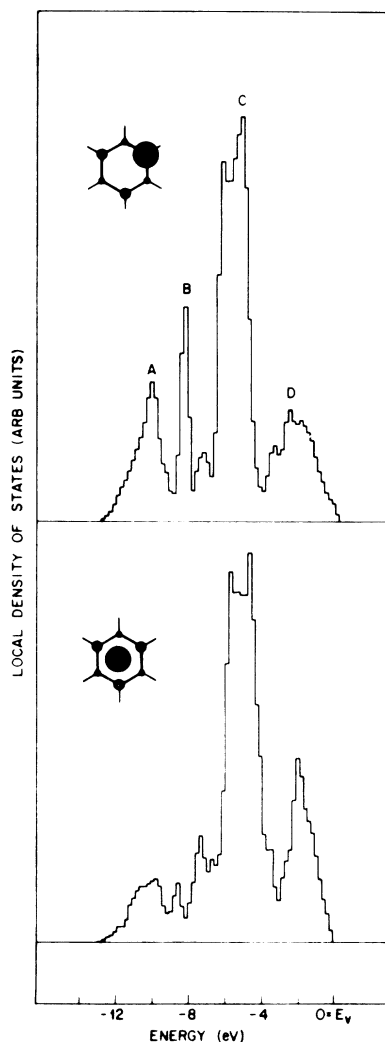


FIG. 1. Calculated local-density-of-states histograms for a Si(111) surface region containing one Si substrate layer and one Cl adsorbate layer. The upper curve corresponds to the onefold-covalent-site chemisorption bond geometry, whereas the lower curve shows the results for a threefold-ionic-site geometry (see text for additional details).

(111) surface layer which includes only a single silicon atom layer with chemisorbed Cl.

For the onefold covalent site we find four peaks, A, B, C, and D. Peak A is due to Si s states with an enhancement ($\sim 40\%$) and slight narrowing due to overlap of the Cl p_z states. Peak B is due to a directional σ -like bond formed with Cl p_z and Si p_z states for the onefold site. Peak C is due to essentially nonbonding Cl p_x and p_y states (they may also be viewed as π -bonding states) which are split by Cl-Cl interactions for the complete 1×1 periodic monolayer. Peak D corresponds to p -like Si-Si bonds in the substrate which are perturbed by the presence of the Cl atom.

For the threefold ionic site *no* σ bonds exist and the nonbonding peak C is now somewhat broadened and contains all three Cl p states (p_x, p_y, p_z). Because of the surface potential there is an unresolved crystal-field splitting of the p_z orbitals toward *higher energy* (i.e., near -4 eV) compared to the p_x and p_y orbitals. An enhancement of Si-Si bond states corresponding to peak D is also found.

In summary, the main feature which distinguishes the electronic structures for these two geometries is the energy position of the Cl p_z orbitals relative to the Cl p_x and p_y orbitals. In the onefold covalent geometry the chlorine p_z orbitals give rise to a well-separated narrow peak on the high-binding-energy side of the main Cl p_x, p_y peak. In the threefold ionic geometry they occur on the low-binding-energy side of the main peak and do not give rise to a separate peak structure.

We have used polarization selection rule effects as well as photon energy-dependent cross-section effects⁸ and energy distributions to identify the symmetry properties of Cl p orbitals. This procedure is an approximation to a more complete comparison of theory and experiment which will require matrix elements and final-state wave functions to be calculated.¹⁴⁻¹⁶ The experimental data for a 1×1 overlayer of Cl on cleaved Si(111) are shown in Fig. 2 for several photon energies. A comparison between data for cleaved Si(111) and cleaved Ge(111) is shown in Fig. 3 for $\hbar\omega = 26$ eV. For s -polarized photons there is no E_z component of the incident light while for p -polarized photons there is both an E_z and $E_{x,y}$ component. It is trivial to show that the electric dipole selection rules^{14,15} select only s -wave and d -wave components of the final-state wave functions for initial states that are p -like. Furthermore only the s -wave component has strong polarization selection rules if a summation is performed over the

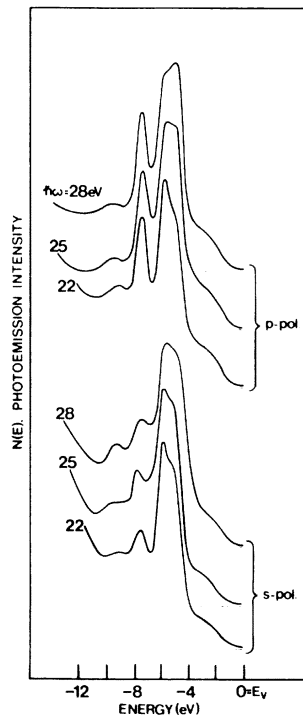


FIG. 2. Experimental photoemission spectra of cleaved Si(111)Cl employing s - and p -polarized photons of energies $\hbar\omega = 22, 25,$ and 28 eV.

five d -wave components. For the s -wave final state the matrix element from p_z initial states is nonzero only for p polarization. Including both s -wave and d -wave contributions will tend to weaken this selection rule. The experimental data for Si(111)Cl in Figs. 2 and 3 show a narrow peak [labeled in Fig. 3(a) by σ_{p_z}] that decreases considerably in intensity for s polarization compared with p polarization. This behavior is predicted for the onefold-covalent-site geometry. However, the Ge(111)Cl data do *not* show such a narrow peak and the only polarization effect is an asymmetric narrowing of the main peak due to an intensity decrease on the low-binding-energy side. This behavior is that predicted for the threefold-ionic-site geometry. The differences between Cl absorbed on Si and Ge is especially striking in view of the strong similarity of both bulk and surface electronic structure. The comparison of theory (Fig. 1) and experiment (Figs. 2 and 3) thus strongly favors the onefold covalent site for Si(111)Cl and the threefold ionic state for Ge(111)Cl. It is quite likely that the onefold and threefold sites occur on other faces of Si and Ge; however, further experimental studies are needed to confirm this prediction.

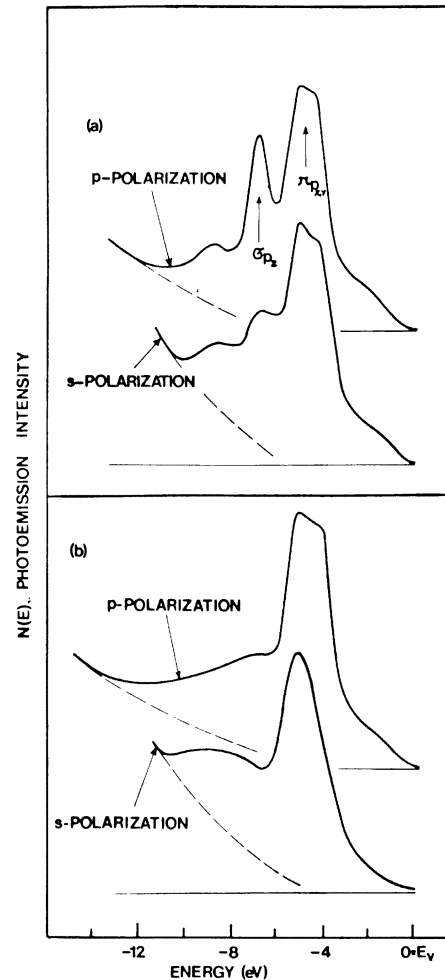


FIG. 3. Experimental photoemission spectra of (a) cleaved Si(111)Cl and (b) cleaved Ge(111)Cl employing s - and p -polarized photons of energy $\hbar\omega = 26$ eV. Note the strong narrow peak near -7 eV (labeled σ_{p_z}) in the Si(111) spectrum. In the Ge(111) spectrum the Cl p_z orbitals seem to occur at higher energies near -4 eV as expected for the threefold-ionic-site geometry.

†Work at the Synchrotron Radiation Center is supported by the National Science Foundation under Grant No. DMR-74-15089.

*Fellow of the Gruppo Nazionale di Struttura della Materia del Consiglio Nazionale delle Ricerche.

¹K. C. Pandey, T. Sakurai, and H. D. Hagstrum, Phys. Rev. Lett. **35**, 1728 (1975).

²H. Ibach and J. E. Rowe, Surf. Sci. **43**, 481 (1974).

³T. Sakurai and H. D. Hagstrum, Phys. Rev. B **12**, 5349 (1975).

⁴J. A. Appelbaum and D. R. Hamann, Phys. Rev. Lett. **34**, 806 (1975); K. M. Ho, M. Schluter, and M. L. Cohen, to be published.

⁵H. Ibach and J. E. Rowe, Phys. Rev. B **10**, 710 (1974).

⁶J. E. Demuth and D. E. Eastman, Phys. Rev. B **13**,

1523 (1976).

⁷M. Schluter, J. R. Chelikowsky, S. G. Louie, and M. L. Cohen, Phys. Rev. B **12**, 4200 (1975).⁸T. Gustafson, E. W. Plummer, D. E. Eastman, and J. L. Freeouf, Solid State Commun. **17**, 391 (1975).⁹J. E. Rowe, Phys. Rev. Lett. **34**, 398 (1975), and Surf. Sci. **53**, 461 (1975).¹⁰Physics Electronics Industries, model No. 15-250, Eden Prairie, Minn.¹¹F. Forstmann, W. Berndt, and P. Buttner, Phys.Rev. Lett. **30**, 17 (1973).¹²G. Rovida, F. Pratesi, M. Maglietta, and E. Feroni, Jpn. J. Appl. Phys., Suppl. **2**, 117 (1974).¹³I. V. Abarenkov and V. Heine, Philos. Mag. **12**, 528 (1965).¹⁴I. Adawi, Phys. Rev. **134**, A788 (1964).¹⁵P. J. Feibelman and D. E. Eastman, Phys. Rev. B **10**, 4932 (1974).¹⁶S. Y. Tong and M. A. Van Hove, Solid State Commun. **19**, 543 (1976), and references cited therein.

Donor Exciton Satellites in Cubic Silicon Carbide: Multiple Bound Excitons Revisited

P. J. Dean, D. C. Herbert, D. Bimberg,* and W. J. Choyke†
 Royal Signals and Radar Establishment, Malvern, Worcestershire, England
 (Received 30 August 1976)

We report a new series of bound-exciton lines just below the associated luminescence of single excitons bound to the shallow donor N_C . The spectral position, Zeeman effect, and behavior under optical pumping indicate origin similar to a satellite series in Si, initially attributed to recombination within multiple bound-exciton complexes at neutral donors and acceptors. We find the multiple bound-exciton model consistent with the properties of these satellite lines both in SiC and in Si, in contrast with recent claims.

The near-gap low-temperature photoluminescence spectra of the best-available-quality cubic SiC (β -SiC) are dominated by a series of related sharp and moderately sharp lines. The highest-energy component is a single line lying ~ 10 meV below the exciton band gap E_{gx} due to the no-phonon (NP) recombination of an exciton bound to a shallow neutral donor, most probably N_C .¹ We refer to this line as the principal bound exciton (PBE) for this donor. The most significant of the related, lower-energy lines result from phonon-assisted transitions in which momentum-conserving phonons (MCP) predominate. In this Letter, we are concerned with a new series of lines, observed equally well as satellites of the NP and MCP lines, covering an energy range of ~ 30 meV below each of them.

The new satellites, $n=2-6(?)$ in Fig. 1(a), were most significant at high excitation intensities (Fig. 2), facilitated in our measurements by a short-focal-length lens for the laser exciting light and the relatively small penetration depth ($\sim 5 \mu\text{m}$) of the ~ 360 -nm light from a Coherent Radiation CR12 laser.² The crystals were cooled by direct immersion in liquid He, pumped below the λ point. Zeeman spectra [Fig. 1(a)] were obtained using a 10-MW Bitter magnet, operated in the Faraday configuration. Only the strongest satellite, $n=2$, has been reported previously; it is the B bound exciton of Hartman and Dean.¹ The Zeeman behavior is similar to a neutral acceptor-

bound exciton. However, intercomparison of crystals showed that the B ($n=2$) exciton became relatively *weaker* with increasing compensation by such likely shallow acceptors as B or Al. Acceptor-bound excitons have yet to be recognized in cubic SiC.

These Zeeman properties in cubic SiC [Fig. 1(a)] are very similar to those given in a recent report for Si:P.³ At low magnetic fields, the number of magnetic subcomponents of the satellites and the PBE are the same, although their relative intensities are very different, appearing to suggest "less thermalization in the transition excited states for increasing n ."³ This qualitative similarity in the Zeeman properties, independent of n , played a key role in the rejection of the multiple-bound-exciton (MBE) model.³ Other inherent features of the MBE model, particularly the *increase* in exciton localization energy E_{BX} for each *additional* exciton bound, also seemed implausible. We now show that these difficulties, as well as some previously disregarded apparent problems with the MBE model, can be resolved within the framework of this model.

One of us⁴ has recently shown that in the absence of ground-state degeneracy, correlation effects play a strong role in the binding of electrons and holes in exciton complexes such as those in Fig. 1(b). When $m_e \sim m_h$, as in both Si and cubic SiC, the exciton localization energy E_{BX} is $\sim 0.44E_D$, where E_D is the donor binding ener-